

Postprint of: Pieczyńska A., Ossowski T., Bogdanowicz R., Siedlecka E., Electrochemical degradation of textile dyes in a flow reactor: effect of operating conditions and dyes chemical structure, International Journal of Environmental Science and Technology, Vol. 16, iss. 2 (2019), pp. 929-942, DOI: [10.1007/s13762-018-1704-0](https://doi.org/10.1007/s13762-018-1704-0)

Electrochemical degradation of textile dyes in a flow reactor: Effect of operating conditions and dyes chemical structure

Electrochemical degradation of textile dyes in a flow reactor

Aleksandra Pieczyńska^{a*}, Tadeusz Ossowski^b, R. Bogdanowicz^c, Ewa Siedlecka^a

^a Department of Environmental Technology, Faculty of Chemistry, University of Gdańsk, 63 Wita Stwosza Str., 80-308 Gdańsk, Poland

^b Department of Analytical Chemistry, Faculty of Chemistry, University of Gdansk, 63 Wita Stwosza Str., 80-308 Gdansk, Poland

^c Department of Metrology and Optoelectronics, Faculty of Electronics, Telecommunications and Informatics, Gdansk University of Technology, 11/12 G. Narutowicza Str., 80-233 Gdansk, Poland,

*Corresponding author : aleksandra.pieczynska@ug.edu.pl

Abstract

In this study, electrochemical oxidation of five azo dyestuffs (Yellow D-5GN, Red D-B8, Ruby F-2B, Blue D-5RN, Black DN), that are widely used in the textile industry was investigated in a flow reactor. BDD electrode with a high boron doping level ($C/B=10\ 000$) was prepared and used. Two configurations of reactor were considered, i.e. one with the undivided cell, and the other with the cell divided by anodic and cathodic compartments. The effect of current density and the initial pH of the solution on the dyestuff degradation process was investigated. As expected, higher degradation rate was found for higher current density, while the effect of pH was marginal. Next, electrochemical oxidation of azo dyestuffs with different chemical structures were investigated. Based on the cyclic voltammetry measurements, the correlation between the dyestuff removal rate and the oxidation potential value of dyestuff was found. These results suggest that the direct oxidation of dyestuffs at the highly doped BDD anode plays a significant role in the electrochemical oxidation. Finally, the electrochemical removal of dyestuffs was carried out in two types of dyeing baths. The dyeing bath composition has a significant effect on the degradation efficiency. Chlorides in F type dyeing bath accelerated electrochemical removal due to effective generation of $Cl_2/HOCl$ at the highly B doped BDD anode. In contrast, OH^- inhibited the D type dyestuff removal from dyeing bath, because they acted as scavengers of $\bullet OH$ radicals. Highly B doped BDD anode is promising material to F type dyestuff treatment in industrial wastewater.

Keywords: Electrochemical degradation, flow reactor, BDD, dyes, effluents

1. Introduction

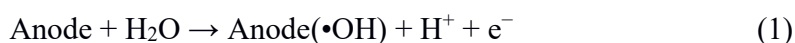
Synthetic dyestuffs are widely used in various types of industries, but mainly in textile industry and paper production (Martínez-Huitle and Brillas, 2009). Dyestuffs can be classified into several groups based on their chemical structure. From among all colorants, azo dyes are the most commonly used, with their manufacture constituting around 70% of total dyestuffs production. These dyestuffs are large molecules possessing at least one $-N=N-$ group (azo-dyes) and one or more functional groups such as $-SO_3H$, $-COOH$, $-OH$, $-NH_2$ and $-NR_2$ (Santos et al., 2008). The functional groups are responsible for the better solubility of these compounds in water as well as increasing the color intensity and ability to bind the colorant to fibers. In response to the consumers expectations, the dyes used for textile dyeing are stable under sunlight, resistant to complete biological degradation, and in many cases, display bacteriostatic properties. Unfortunately, if they are decomposed, some of their transformation products, e.g. aromatic amines can be toxic and even mutagenic (Basha et al., 2012).

Textile industry (dyeing and finishing processes) is characterized by a high demand for water which, in turn, generates the large volumes of wastewater containing the dyestuff residues (Santos et al., 2008). The textile wastewater is characterized by strong color, because even 15% of used dyestuffs end up in it. Such wastewater contains high concentrations of organic compounds which frequently translates into very high chemical oxygen demand (COD). The pH values of textile wastewater vary from 2 to 12 due to the composition of dyeing baths (Oller et al., 2011; Wächter et al., 2015). The environmental legislation obliges the industries to eliminate COD, total nitrogen and specific color from their dye-containing effluents prior to their disposal into the water bodies (O'Neill et al., 1999). However, the effective textile wastewater treatment is frequently problematic. Numerous reports indicate that many compounds used in dyeing baths are not effectively decomposed/removed in conventional wastewater treatment plants (El-ghenymy et al., 2014).

A variety of different approaches has been applied in order to remove the dyestuffs from wastewater, e.g. biological methods, adsorption, photocatalytic processes, membrane filtration, and electrochemical methods (Martínez-Huitle and Brillas, 2009). Recently, an increased interest in electrochemical oxidation, including decolorization of textile wastewater, was observed. This can be connected to the fact that electrochemical techniques are already being used in textile processes



such as manufacturing fibers, dyeing processes and decolorizing fabrics. The electrochemical processes are characterized by high energy efficiency and versatility, and can be easily automated (Martínez-Huitle and Ferro, 2006; Panizza and Cerisola, 2009). Moreover, the processes are carried out under mild conditions, such as normal pressure and temperature, while electrons as the main reagent. Therefore, the electrochemical processes are regarded as safe and environmentally friendly techniques. Most of electrochemical oxidation processes involve indirect reactions which imply the *in situ* generation of hypochlorite or hydroxyl radical. These oxidants can effectively react with organic compounds. The other way to oxidize the dyestuffs is via direct charge transfer from anode surface to organic compound, but in some cases this process is less effective (Martínez-Huitle and Brillas, 2009; Panizza and Cerisola, 2009) and characteristic for the “active” electrodes :



This process is marginal at the “non-active “ electrodes e.g. BDD. The efficiency of electrolysis depends on many different parameters such as current density, type and concentration of contaminants, and, primarily, the anode material. Recently, much interest has been focused on the boron-doped diamond (BDD) thin film as a possible anode material (Brillas, 2014). Such electrode is characterized by the surface with low affinity to organic matter and extremely high O₂ evolution overvoltage results in powerful •OH radicals generation and in presence of chlorides relatively low Cl₂/HClO production (Luong et al., 2009; Panizza and Cerisola, 2009). Additionally, it was reported that BDD is powerful enough to mineralize aromatic compounds such as dyestuffs (R. Bogdanowicz et al., 2013; Santos et al., 2008; Wächter et al., 2015), chemically resistant imidazolium ionic liquids (Fabiańska et al., 2012; Pieczyńska et al., 2015), and micropollutants, including pesticides (Samet et al., 2010) and pharmaceuticals (Fabiańska et al., 2014, 2013). However, the efficiency of electrochemical process at the BDD electrode depends, among others, on the boron doping level in the diamond material. The boron doping level has an effect on the crystalline structure and layer conductivity of BDD electrode. Higher amounts of dopant on the surface of Si/BDD resulted in the higher conductivity of thin film electrode. The study by Feng et al. (2011) on phenol oxidation demonstrated that with increasing level of boron in the BDD electrode, the electrolysis time decreases and the anodic peak shifts to lower potential range. The electrochemical dyestuff oxidation was usually study at commercial BDD anodes with the B/C ratio of 500 ppm. The highly B doped diamond material as an anode in dyestuff treatment has not been yet studied.

Another important factor influencing the efficiency of pollutant decomposition is the type of electrochemical system applied. Different options of electrochemical systems, such as bath or flow reactors and reactors with separate anodic and cathodic compartments, have been tested for treatment of dyestuff solutions (Basha et al., 2012; El-Ghenymy et al., 2014; Wächter et al., 2015). The hydrodynamics of the cell plays an important role in the mass transport to electrodes and the oxidation efficiency of organic pollutants. El-Ghenymy et al. reported on the higher degradation efficiency of pollutants in a cell divided into anodic and cathodic compartments in comparison to the process conducted in an undivided cell. This phenomenon resulted from a better mass transport and higher concentration of generated oxidants in the anodic space (El-Ghenymy et al., 2014). Furthermore, the process carried out in a divided cell limited the side reactions at the anode surface as well as decreased the reduction processes of some intermediates at the cathode. Basha et al. (2012) compared the COD removal efficiency and energy consumption for the electrochemical oxidation processes carried out in a bath reactor with and without recirculation of effluents. The aforementioned studies have shown that the application of a reactor with recirculation ensures better results. However, the reports on the testing of a flow reactor divided into anodic and cathodic spaces are still rather sparse.

In the present study, the electrochemical oxidation of five helactine azo dyestuffs (Table 1) was investigated by means of i) the BDD electrode with a high boron doping level (as prepared by us) and ii) a reactor divided into cathodic and anodic spaces with a Nafion - cation exchange membrane. The results were compared with those obtained in a flow reactor with an undivided cell. The helactive azo dyestuffs have been selected because they represent about 20–30% of the total dye market (Carneiro et al., 2005), due to their brilliant colors. They are widely used in the textile industry for dyeing cellulose fibers. The influence of the current density, initial pH and the initial concentration of dyestuffs was investigated in detail. The fact that the dyeing process requires specialized technology has also been taken into consideration. Therefore, the studies not only include the electrochemical oxidation of the dyestuff solution, but also examine synthetic mixtures simulating the composition of real textile wastewater generated in dyeing process. Furthermore, a possible reaction and the electrogenerated intermediates of dyestuffs were identified and discussed. According to our knowledge, the electrochemical decomposition of selected dyestuffs at the BDD electrode with a high doping level in a flow reactor has not yet been studied.

2. Materials and methods

2.1. Materials

Five azo dyestuffs commonly used in the textile industry, namely, Yellow D-5GN, Red D-B8, Ruby F-2B, Blue D-5RN and Black DN, were selected for testing. The dyes were obtained from BORUTA S.A., a Polish company producing dyestuffs. The chemical structures of dyestuffs are shown in Table 1. Sodium sulfate, sodium chloride, acid sulfate, sodium hydroxide and sodium carbonate were purchased from STANLAB (Lublin, Poland).

2.2. Electrode preparation

The BDD electrode was synthesized on p-type Si wafers in a microwave plasma-assisted chemical vapor deposition (MW PA CVD) system (Seki Technotron, AX5400S, Japan) where the [B]/[C] ratio in plasma was 10 000 ppm. Diborane (B₂H₆) was used as boron precursor. The electrode was characterized by resistivity and electrochemical activity via cyclic voltammetry (CV). The preparation and characterization of the BDD electrode were both described in detail by R. Bogdanowicz et al. (2013).

2.3. Electrochemical experiments

Cyclic voltammetry (CV) was carried out on a potentiostat/galvanostat PGSTAT-30Autolab, using a scan rate of 100 mV s⁻¹. A BDD electrode of the surface area 0.28 cm² was used as the working electrode, platinum wire as the counter electrode, and Ag/AgCl/0.1 M KCl electrode as the reference electrode. The concentrations of dyestuff in supporting electrolyte (SE) (Na₂SO₄, 6 g L⁻¹) were in range from 0.5 to 6 mM. All experiments were performed at room temperature (25 ± 2 °C) in a bath reactor with a volume of 3 mL. Prior to the experiments, all BDD electrodes were cathodically pre-treated in a 0.5 M H₂SO₄ solution by applying - 1.0 A cm⁻¹ for 120 s.

The electrochemical decomposition experiments were carried out in a flow reactor that had been designed and constructed by our scientific team (Fig.1.). The electrolytic cell of reactor was divided with a Nafion -cation exchange membrane into anodic and cathodic spaces. BDD/Si, and stainless steel plates with a surface area of 2.3 cm², were used respectively as anode and cathode. A Manson NSP-3630 device was used as power supply. The recirculation flow of 0.6 L h⁻¹ was provided by peristaltic pumps (Elpan 372C) and the processed volume was 0.1 L in each run. The limiting current density was determined in accordance with Pereira et al. (2012),



The feed solutions of dyestuffs were prepared in supporting electrolyte (Na_2SO_4 , 6 g L^{-1}) and in synthetic wastewater simulating the composition of real textile wastewater from dyeing processes. The wastewater was prepared in accordance with the textile industry guide BN-86 6041-19. In the case of helactine F dyestuff (Ruby F-2B), the dyeing bath consisted of aqueous solution of sodium chloride (60 g L^{-1}), sodium carbonate (4 g L^{-1}) and dyestuff (50 mg L^{-1}) at pH 9. In relation to helactine D dyestuffs (Yellow D-5GN, Red D-B8, Blue D-5RN, Black DN), an aqueous solution of sodium chloride (80 g L^{-1}), sodium carbonate (20 g L^{-1}), sodium hydroxide 32.5 % (3 ml L^{-1}) and dyestuff (50 mg L^{-1}) at pH 12 was used.

The effects of the initial pH of the solution (from 3.0 to 12.0), current density ($3.5 - 8.8 \text{ mA cm}^{-2}$), dyestuff concentration (10 to 50 mg L^{-1}) and dyestuff chemical structure on the kinetics of electrochemical oxidation and dyestuff removal efficiency were investigated by using five dyestuffs (Yellow D-5RN, Red D-B8, Ruby F-2B, Blue D-5RN and Black DN).

2.4. Analysis

UV-Vis Spectrophotometer (Thermo Scientific, Evaluation 220) was used to monitor the decomposition rate of dyestuffs and the absorbance spectrum. The Chemical Oxygen Demand (COD) was measured by using standard cuvette test. The current efficiency (CE) for electrochemical oxidation of dyestuffs was calculated by using the following equation (Brillas, 2014):

$$CE\% = \frac{FV(COD_t - COD_0)}{8000I\Delta t} \times 100$$

where I is the applied current (A), Δt is time of the process (s), V is the solution volume (L), F is the Faraday constant (96485 C mol^{-1}), and COD_0 and COD_t are the experimental chemical oxygen demands ($\text{mgO}_2 \text{ L}^{-1}$).

According to Siedlecka et al. (2013), the amount of $\bullet\text{OH}$ radicals was determined by using 0.1 L of 0.03 mM N,N -dimethyl- p -nitrosoaniline (RNO) solution in phosphate buffer (pH 7.1). The changing absorbance of RNO solution at $\lambda = 440 \text{ nm}$ during the electrochemical process was proportional to $\bullet\text{OH}$ concentration, and was calculated from the equation:

$$[\bullet\text{OH}] = 1 - \frac{[\text{RNO}]_t}{[\text{RNO}]_0}$$

where $[·OH]$ is the hydroxyl radical amount, $[RNO]_0$ and $[RNO]_t$ are the concentrations of N,N-dimethyl-p-nitrosoaniline initially and in time t , respectively.

3. Results and discussion

3.1. Characterization of electrode

As a result of the incorporation of boron atoms into the diamond lattice, the Si/BDD electrode with high doping level (B/C ratio of 10 000 ppm) was characterized by relatively low resistance (7 m Ω cm), the average grain size (76%) smaller than 1 μ m, and high electroactivity (R Bogdanowicz et al., 2013). The O₂ evolution overvoltage on the prepared BDD was 1.5 V (data not shown), which is quite a low value compared to the commercial BDD electrodes obtained from Adamant Technologies with the B/C ratio equal 500 ppm ($E \sim 2.3$ V) (Siedlecka et al., 2013). These results suggest that the prepared BDD electrode is able to generate the \bullet OH radicals, while the direct oxidation process is also possible.

3.2. Electrochemical degradation of dyestuff for two configurations of flow reactor

Preliminary the limiting current density and the optimal flow rate were performed. In order to compare the efficiency of dyestuff removal in the divided and undivided cell of flow reactor the same experimental conditions were used in both configurations of reactor. The electrochemical oxidation of Ruby F-2B (20 mg L⁻¹) solution in Na₂SO₄ electrolyte was carried out at a current density of 8.8 mA cm⁻² (higher than the limiting current density) and flow rate of 0.6 L h⁻¹. The results are presented in Figure 2.

As can be seen, after a 120-min process, 94 % of the initial dyestuff concentration was removed in the divided cell. During the same time period, only 55 % of the initial dyestuff amount was degraded in the undivided cell. In both cases, the plots of the dyestuff concentrations versus time fitted well to a pseudo-first-order reaction. The degradation rate coefficient k value in two compartments reactor was 3.13 times higher ($k = 2.1 \times 10^{-2}$ min⁻¹, $R^2 = 0.9733$) than that obtained in one compartment reactor ($k = 0.67 \times 10^{-2}$ min⁻¹, $R^2 = 0.9987$). Similar trend in degradation rate of organic matter have been reported by El-Ghenymy et al. (2014) who investigated the electrochemical oxidation of sulfanilamide and Orange G in the divided and undivided cell of reactor. The presented results can be explained by a higher oxidation ability at the BDD electrode in the two compartments reactor, due to limited cathodic reaction with some degradation

intermediates and oxidizing entities generated simultaneously with the $\bullet\text{OH}$ radicals at the BDD anode. The oxidants which simultaneously could be formed under our experimental conditions are $\text{S}_2\text{O}_8^{2-}$ and O_3 . However they are the weaker oxidants than $\bullet\text{OH}$ radicals. The higher efficiency of the reaction of $\bullet\text{OH}$ radicals with organic compounds in divided cell reactor could be result the presence of Nafion membrane that due to the increased the electrochemical potential had a major influence on the mass transport toward the anode (El-Ghenymy et al., 2014). The higher efficiency and faster dyestuff degradation was achieved with the divided cell reactor were the basic reasons for applying this set-up in further studies.

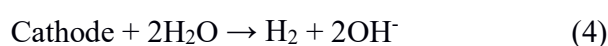
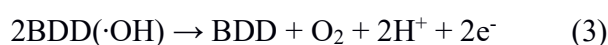
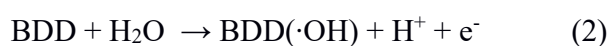
3.3. Effect of applied current density in divided cell flow reactor

The applied current density is main parameter, which regulates the amount of reactive $\bullet\text{OH}$ radicals produced at the BDD anode and the energy waste due to side reactions. Therefore, the values of current density: 3.5, 6.6 and 8.8 mA cm^{-2} used in our investigations to electrochemical degradation of Ruby F-2B (20 mg L^{-1}) was in each case higher than limiting current density, and the process was controlled by mass transport. The experiments were performed in the divided cell flow reactor fed by the dye solution in Na_2SO_4 electrolyte at pH 3. The pseudo-first order rate constants k equal to 2.10×10^{-2} ($R^2 = 0.9733$), 0.92×10^{-2} ($R^2 = 0.9880$) and 0.59×10^{-2} ($R^2 = 0.9907$) min^{-1} were calculated for the current density values of 8.8 mA cm^{-2} , 6.6 mA cm^{-2} , 3.5 mA cm^{-2} , respectively. As expected, the rate coefficient increased with the elevation of current density (Fig 3b). A similar relationship was reported by other researchers in the case of pollutant degradation in the divided reactor with the BDD electrode (El-Ghenymy et al., 2014, 2012). However, as can be seen in Fig. 3C, for the same specific charge Q flown through the cell at different current density, the same amount of hydroxyl radicals was produced. This indicates that the generation efficiency of $\bullet\text{OH}$ radicals via electrochemical process at BDD anode was independent of the current density used. The advantage of flow reactor is fact that despite the increasing value of current density, the energy waste remained the same. This phenomenon is characteristic for the mass transfer controlled processes, as has also been observed by Velegraki et al. (2010) However, at the higher current density less time was needed to decompose the dye, therefore in further investigations the value of 8.8 mA cm^{-2} was chosen as optimal current density .

3.4. Effect of initial pH

The role of initial pH in the oxidation of Ruby F-2B in solution of 20 mg L⁻¹ at the BDD anode surface was studied for the pH values of 3.0, 7.0, 9.0 and 12.0. The electrochemical degradation was carried out in the divided cell at a current density of 8.8 mA cm⁻². The obtained results are presented in Fig. 4. In this study, the influence of pH on the oxidation of dyestuff was marginal. In all cases (initial pH 3.0 – 12.0), the almost total decomposition of the dyestuff occurred after 150 min.

It is noteworthy that the electrolysis at all initial pH values caused rapid acidification of the solutions (pH < 2.0), due to the lack of neutralization of proton generated at the anodic compartment (reaction (2)-(3) by ⁻OH⁻ anions generated at the cathodic space (reaction 4) (El-Ghenymy et al., 2013).



The pH value of the solution significantly influenced the degradation efficiency in the undivided electrochemical cell, what was reported by Fabiańska et al. (2014) and Palma-Goyes et al. (2010). The difference in rate of organic matter degradation at various pH is frequently connected with the higher redox potential of hydroxyl radicals under acidic conditions compared to alkaline environment. However in divided cell flow reactor after 15 min. of electrolysis, independently of initial pH, pH value of solution was about 2. On the other hand, COD or TOC removal efficiency did not depend on pH (Palma-Goyes et al., 2010; Pereira et al., 2012).

3.5. Effect of chemical structure on the electrochemical degradation rate of dyestuffs

The cyclic voltammetric measurements of dyestuff solutions showed that all dyestuffs were directly oxidized at the surface of BDD electrode. The oxidation potentials of dyestuffs were 0.75, 0.99, 1.06, 1.11 and 1.16 V for Blue D-5RN, Yellow D-5GN, Red D-8B, Ruby F-2B and Black DN, respectively (Table 2). These results indicate that Blue D-5RN was most prone to direct oxidation, while Black DN was the most electrochemically resistant.

The investigation of galvanostatic electrochemical degradation was carried out in the solutions of selected dyestuffs at their initial concentration of 50 mg L⁻¹. The experiments were performed in



the divided cell flow system under the following conditions: current density 8.8 mA cm^{-2} , flow rate 0.6 L h^{-1} , and pH 3.0. Figure 5 shows the variation of dyestuff concentrations as a functions of time, and in Table 2, the values of rate constant of the dyestuff decomposition, COD removal efficiency and current efficiency of electrochemical oxidation of dyestuffs are listed.

The rate coefficients of dyestuffs degradation decrease in the following order: $k(\text{Blue D-5RN}) > k(\text{Yellow D-5GN}) > k(\text{Red D-8B}) > k(\text{Ruby F-2B}) > k(\text{Black DN})$. The results clearly indicate that k of dyestuffs were directly proportional to their oxidation potentials. The Blue D-5RN with the lowest oxidation potential was more easily decomposed under galvanostatic conditions, while the Black DN with the highest oxidation potential was most resistant. This fact suggests that the direct oxidation of dyestuffs could play a role in their electrochemical removal at the BDD anode with the highly boron doped level.. The applied BDD electrode was more selective towards the direct oxidation of organic matter than the BDD electrodes with the low B/C ratio. The latter aforementioned anode degraded the organic matter by producing high amounts of non-selective $\bullet\text{OH}$ radicals (R Bogdanowicz et al., 2013; Fabiańska et al., 2013) and the direct oxidation of pollutants at anode surface was limited

In Figure 6, UV-Vis spectra of electrochemically decomposed dyestuffs over time are presented. As can be seen, for all the analyzed dyestuffs, the intensity of peak characteristic for the azo bond decreased in electrolysis time. In the case of Black DN, the decreasing of intensity of peak assigned to the naphthalene rings was proportional to the decreasing of intensity of peak attributable to the azo bonds. For Yellow D-5GN, Red D-8B and Ruby F-2B, the intensity of peak of naphthalene rings was lower than the intensity of peak of azo bonds. Furthermore, any significant changes in the shape of absorbance spectra were not observed. A different behavior was observed in the case of Blue D-5RN where the peak characteristic for the naphthalene rings was found after 1 h of the process, while the peak associated with the azo bonds disappeared. This fact suggests that the hydroxyl-naphthalene intermediates probably formed during the electrochemical oxidation, and the azo bonds were destroyed faster than the naphthalene rings. In the case of Blue D-5RN, the naphthalene rings are substituted by different functionalities making them more resistant for oxidative cleavage. It can be concluded that the decomposition rate of the dyestuff and generated intermediates depend on the amount of substituents in the naphthalene ring. However, it is difficult to clearly determine the effect of each substituent on the degradation process. Sanroman et al.

(2004) conducted the study of the electrochemical oxidation of dyestuffs using Pt electrode which showed that the decomposition rate depends on the nature and number of the substituents of phenyl groups and the complexity of the substituents of the aromatic rings. Considering the structure of selected dyestuffs in relation to the decomposition rate and degradation efficiency, no clear correlation between the amount and the nature of substituents of the aromatic rings was found. In such complex structures, several factors affect the degradation rate simultaneously, which was previously reported by Santos et al. (2008). Different behavior displayed by D-5RN compared to other dyes can be possibly explained by the low redox potential and higher participation of direct oxidation at the surface of BDD electrode during decomposition. However, further investigations should be carried out to elucidate this phenomenon.

The oxidation of organic matter via electrolysis was monitored by COD measurements. As shown in Table 2, the COD removal efficiency reached almost 100% for all the analyzed dyes, however, the reaction time varied. For example, the removal of 99.1% of COD for Blue D-5RN was achieved in 120 min, while the removal of 93.4% of COD for Black DN was reached after 480 min.. The rates of COD removal were in the following order: $k(\text{Blue D-5RN}) > k(\text{Yellow D-5GN}) > k(\text{Red D-8B}) > k(\text{Ruby F-2B}) > k(\text{Black DN})$. The results clearly indicate that COD removal rates correlated with the redox potential of the analyzed dyes. This finding proves that the dyes and their intermediates were degraded simultaneously via direct and indirect processes.

The current efficiency (CE) values for the electrochemical degradation of dyestuffs in the divided cell flow reactor are presented in Table 2. The highest CE value (92.1%) was obtained for the removal of Blue D-5RN. In the case of Yellow D-5GN, Red D-8B, Ruby F-2B and Black DN, the respective CE values were 60.9, 37.5, 25.2 and 22.1%. The high CE is advantageous because of the low waste of energy in side reactions, such as generation of hydrogen peroxide (reaction (5)), or evolution of oxygen.

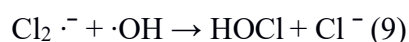
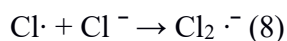
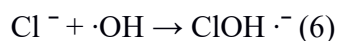


The CE values obtained for the decomposition of dyestuffs were also proportional to their direct oxidation potentials.

3.6. Degradation efficiency of dyestuffs in dyeing bath wastewater

Dyeing bath wastewaters are characterized by specific composition and strong colors, and usually display high COD values, high conductivity and alkaline pH (Basha et al., 2012; Tsantaki et al., 2012). The presence of high concentration of inorganic salts makes the electrochemical oxidation the appropriate method for treating this type of wastewater. In order to check how the composition of dyeing bath wastewater affects the electrochemical degradation efficiency of dyestuffs, helactine dyestuffs from group F and group D were used to prepare simulated wastewaters in accordance with the Polish norm for the dyeing process. It is worth mentioning that many authors (Basha et al., 2012; Yavuz et al., 2007), have not investigated the effect of dyeing bath on the electrochemical degradation efficiency of textile wastewater. The dyeing bath compositions for the dyes from group F and group D differ with regard to the content of sodium chloride and sodium carbonate. The higher content of both compounds is used in dyeing bath for group D than in dyeing bath for group F. The electrochemical decomposition of the analyzed dyestuffs in dyeing baths is presented in Figure 7.

A high increase in the degradation rate of Ruby F-2B in dyeing bath (group F) compare to degradation rate of this colorant in supported electrolyte was observed. In dyeing bath wastewater, this dyestuff underwent complete decomposition within 15 min, while the same process took 7 hrs in an electrolyte solution (6g of Na_2SO_4). Such rapid decomposition of Ruby F-2B in dyeing bath wastewater can be explain by the presence in dyeing bath of chloride ions, which react with the hydroxyl radicals forming different active chlorine species according to the reactions (6) - (10) (Bruguera-Casamada et al., 2017; Moreira et al., 2017; Muruganathan et al., 2011). These species can effectively degrade organic pollutants, including dyestuffs. The existence of particular chlorine species in the solution is pH dependent. The Cl_2 species is predominant at a pH less than 3, HClO is the main form in the pH range 3-8, while ClO^- exists at the pH values higher than 8. The oxidation of organics with the aforementioned chlorine species is faster in acidic medium than in alkaline medium due to the higher standard potential of Cl_2 ($E = 1.36 \text{ V}$) and HClO ($E = 1.49 \text{ V}$) compared to ClO^- ($E = 0.89 \text{ V}$). The decomposition of Ruby F-2B in dyeing bath wastewater increased because the initial pH value of 9 dropped down to 3 within the first 15 min of electrolysis, due to remove $\text{HCO}_3^-/\text{CO}_3^{2-}$ ions that appear as $\bullet\text{OH}$ scavengers. That was advantageous in relation to the formation of chlorine species, i.e. HClO that are more reactive with dyestuffs and other organic matter.



In the case of other dyestuffs, the electrochemical oxidation in dyeing bath wastewater was not as fast as for Ruby F-2B, despite the presence of high concentration of chloride ions. Moreover, the results obtained for Blue D-5RN, Yellow D-5GN, Red D-8B and Black DN did not fit the kinetics of pseudo-first order reaction. In contrast to the decomposition of dyestuffs in Na_2SO_4 electrolyte, the plot of $\ln(C/C_0)$ versus time for the decay of dyestuffs from group D in wastewater was not linear ($R^2=0.63-0.88$). The two stages of reaction were observed, i.e. a slow removal of dyestuffs followed by the accelerating oxidation process. The observed difference in the reaction kinetics may be associated with the complexity of wastewater matrix. All components present in dyeing bath wastewater can (i) react with the hydroxyl radicals which inhibits the dyestuff oxidation, and/or (ii) undergo direct oxidation at the BDD surface (Fabiańska et al., 2015) which generates free radicals accelerating the dyestuff oxidation process. For example, the high amount of carbonate and bicarbonate ions can scavenge the hydroxyl radicals and thus limit the oxidation of organics (Moreira et al., 2017). On the second hand, these ions can generate percarbonate oxidants at the BDD electrode. Percarbonates are poor oxidants in comparison to dichlorine radicals and other active chlorine species. Additionally, the acidic conditions are advantageous for the organic matter oxidation by these chlorine species therefore the scavenging effect of carbonate and bicarbonate on hydroxyl radicals is limited.

The slower decomposition of dyestuffs from group D compared to group F can be explained by the high initial pH of the dyeing bath wastewater. In this case, the initial pH was 12 because of the high concentration of NaOH in the solution. During the electrolysis, pH was decreasing due to continuous generation of H^+ at the anode surface in accordance with reaction (2). However, in the case of dyestuffs from group D, the concentration of NaOH was so high that the pH value after the electrolysis dropped down only to 9. Therefore, the electrochemical oxidation of organics in the presence of active chlorine species under alkaline conditions (ClO^-) was slower than that in acidic



conditions (HOCl) obtained for mixtures after electrolysis of the dyestuff from group F where pH was 3 (Moreira et al., 2017).

Tsantaki et al. (2012), who investigated anodic oxidation of two textile effluents, observed the higher efficiency of TOC and COD removal in effluents with lower pH values. It can be concluded that the effluent matrix has a significant effect on the efficiency of dyestuff degradation, and thus should always be taken into account. Moreover, it is possible that the BDD electrode with the high B/C ratio prepared for this study was more effective at the *in situ* generation of Cl₂/HOCl than the BDD electrodes with the low B/C ratio that are mainly used in the wastewater oxidation. The correlation between the generation of Cl₂/HOCl and the B/C ratio in diamond thin film of the BDD anode should be confirmed by further investigations.

Conclusions

In the present work, the electrochemical oxidation of five azo dyestuffs at the highly B doped BDD electrode (C/B ratio of 10000 ppm) in a flow reactor was investigated. The selected compounds belong to helactine dyes from group F and group D, and are widely used in the textile industry. Two configuration of cell flow reactor were considered, i.e. one with the undivided electrolyte cell, and the other with the anodic and cathodic cell compartments. The results showed a better oxidation ability at BDD anode in the case of undivided cell flow reactor. The effects of the pH of the solution and of current density on the process were investigated. The effect of the initial pH of the solution was marginal in divided cell flow reactor. As expected, the higher degradation rate was found for the higher current density, but the current efficiency remained satisfactory under all studied conditions. Moreover, there was no correlation between the chemical structure and oxidation efficiency, but the direct relation between the oxidation potential value of dyestuff and its degradation rate was found. It was surprised, because the majority oxidants at BDD electrodes are non-selective •OH radicals. This fact was explained by the occurrence of the direct oxidation of dyestuffs during decomposition at prepared by us BDD highly boron doped electrode. Finally, the electrochemical oxidation of dyestuffs was carried out in dyeing bath wastewater. The results showed that the complex composition of such wastewater has a high influence on the rate of dyestuff removal. The presence of chloride ions significantly accelerated the removal of dyestuffs, while the presence of NaOH, which is used in high concentration in dyeing bath for dyestuffs from group D, inhibited this process. It was hypothesized that the BDD electrode with the high B/C ratio

is selective towards the generation of active chlorine species and direct oxidation of dyestuffs like “active” electrodes.

The correlation between the oxidation potential value of dyestuff and its degradation rate demonstrated that the direct oxidation can play significant role in mechanism of dyestuffs electrochemical oxidation.

Acknowledgements

The authors would like to acknowledge the financial support of the Polish Ministry of Science and Higher Education under the grants DS 530-8626-D596-17-1F, BMN 538-8626-B409-16, BMN 538-8375-B402-16 and BMN 538-8626-B64-15. We also want to express our gratitude to Mrs. Paulina Bojko for her help in the laboratory work.

References

- Balci, B., Oturan, N., Cherrier, R., Oturan, M.A., 2009. Degradation of atrazine in aqueous medium by electrocatalytically generated hydroxyl radicals . A kinetic and mechanistic study. *Water Res.* 43, 1924–1934. doi:10.1016/j.watres.2009.01.021
- Basha, C.A., Sendhil, J., Selvakumar, K.V., Muniswaran, P.K. a., Lee, C.W., 2012. Electrochemical degradation of textile dyeing industry effluent in batch and flow reactor systems. *Desalination* 285, 188–197. doi:10.1016/j.desal.2011.09.054
- Bogdanowicz, R., Fabiańska, a., Golunski, L., Sobaszek, M., Gnyba, M., Ryl, J., Darowicki, K., Ossowski, T., Janssens, S.D., Haenen, K., Siedlecka, E.M., 2013. Influence of the boron doping level on the electrochemical oxidation of the azo dyes at Si/BDD thin film electrodes. *Diam. Relat. Mater.* 39, 82–88. doi:10.1016/j.diamond.2013.08.004
- Brillas, E., 2014. 4. BDD electrochemical reactors 661, 59–78.
- Bruguera-Casamada, C., Sirés, I., Brillas, E., Araujo, R.M., 2017. Effect of electrogenerated hydroxyl radicals, active chlorine and organic matter on the electrochemical inactivation of *Pseudomonas aeruginosa* using BDD and dimensionally stable anodes. *Sep. Purif. Technol.* 178, 224–231. doi:10.1016/j.seppur.2017.01.042

- Butrón, E., Juárez, M.E., Solis, M., Teutli, M., González, I., Nava, J.L., 2007. Electrochemical incineration of indigo textile dye in filter-press-type FM01-LC electrochemical cell using BDD electrodes. *Electrochim. Acta* 52, 6888–6894. doi:10.1016/j.electacta.2007.04.108
- Carneiro, P.A., Osugi, M.E., Fugivara, C.S., Boralle, N., Furlan, M., Zanoni, M.V.B., 2005. Evaluation of different electrochemical methods on the oxidation and degradation of Reactive Blue 4 in aqueous solution. *Chemosphere* 59, 431–439. doi:10.1016/j.chemosphere.2004.10.043
- Chen, G., 2004. Electrochemical technologies in wastewater treatment. *Sep. Purif. Technol.* 38, 11–41. doi:10.1016/j.seppur.2003.10.006
- Degaki, A.H., Pereira, G.F., Rocha-Filho, R.C., Bocchi, N., Biaggio, S.R., 2013. Effect of Specific Active Chlorine Species and Temperature on the Electrochemical Degradation of the Reactive Blue 19 Dye Using a Boron-Doped Diamond or DSA Anode in a Flow Reactor. *Electrocatalysis* 5, 8–15. doi:10.1007/s12678-013-0156-z
- El-Ghenemy, A., Arias, C., Cabot, P.L., Centellas, F., Garrido, J.A., Rodríguez, R.M., Brillas, E., 2012. Electrochemical incineration of sulfanilic acid at a boron-doped diamond anode. *Chemosphere* 87, 1126–33. doi:10.1016/j.chemosphere.2012.02.006
- El-Ghenemy, A., Cabot, P.L., Centellas, F., Garrido, J.A., Rodríguez, R.M., Arias, C., Brillas, E., 2013a. Electrochemical incineration of the antimicrobial sulfamethazine at a boron-doped diamond anode. *Electrochim. Acta* 90, 254–264. doi:10.1016/j.electacta.2012.11.125
- El-Ghenemy, A., Centellas, F., Garrido, J.A., Rodríguez, R.M., Sirés, I., Cabot, P.L., Brillas, E., 2014. Decolorization and mineralization of Orange G azo dye solutions by anodic oxidation with a boron-doped diamond anode in divided and undivided tank reactors. *Electrochim. Acta* 130, 568–576. doi:10.1016/j.electacta.2014.03.066
- El-Ghenemy, A., Garrido, J.A., Rodríguez, R.M., Cabot, P.L., Centellas, F., Arias, C., Brillas, E., 2013b. Degradation of sulfanilamide in acidic medium by anodic oxidation with a boron-doped diamond anode. *J. Electroanal. Chem.* 689, 149–157. doi:10.1016/j.jelechem.2012.11.013



- Fabiańska, A., Białk-Bielińska, A., Stepnowski, P., Stolte, S., Siedlecka, E.M., 2014. Electrochemical degradation of sulfonamides at BDD electrode: kinetics, reaction pathway and eco-toxicity evaluation. *J. Hazard. Mater.*
- Fabiańska, A., Bogdanowicz, R., Zięba, P., Ossowski, T., Gnyba, M., Ryl, J., Zielinski, A., Janssens, S.D., Haenen, K., Siedlecka, E.M., 2013. Electrochemical oxidation of sulphamerazine at boron-doped diamond electrodes: Influence of boron concentration. *Phys. Status Solidi* 210, 2040–2047. doi:10.1002/pssa.201300094
- Fabiańska, A., Ofiarska, A., Fiszka-Borzyszkowska, A., Stepnowski, P., Siedlecka, E.M., 2015. Electrodegradation of ifosfamide and cyclophosphamide at BDD electrode: Decomposition pathway and its kinetics. *Chem. Eng. J.* 276, 274–282. doi:10.1016/j.cej.2015.04.071
- Fabiańska, A., Ossowski, T., Stepnowski, P., Stolte, S., Thöming, J., Siedlecka, E.M., 2012. Electrochemical oxidation of imidazolium-based ionic liquids: The influence of anions. *Chem. Eng. J.* 198–199, 338–345. doi:10.1016/j.cej.2012.05.108
- Feng, Y., Lv, J., Liu, J., Gao, N., Peng, H., Chen, Y., 2011. Influence of boron concentration on growth characteristic and electro-catalytic performance of boron-doped diamond electrodes prepared by direct current plasma chemical vapor deposition. *Appl. Surf. Sci.* 257, 3433–3439. doi:10.1016/j.apsusc.2010.11.041
- Luong, J.H.T., Male, K.B., Glennon, J.D., 2009. Boron-doped diamond electrode: synthesis, characterization, functionalization and analytical applications. *Analyst* 134, 1965–79. doi:10.1039/b910206j
- Martínez-Huitle, C. A., Ferro, S., 2006. Electrochemical oxidation of organic pollutants for the wastewater treatment: direct and indirect processes. *Chem. Soc. Rev.* 35, 1324–40. doi:10.1039/b517632h
- Martínez-Huitle, C., Brillas, E., 2009. Decontamination of wastewaters containing synthetic organic dyes by electrochemical methods : A general review. *Appl. Catal. B Environ.* 87, 105–145. doi:10.1016/j.apcatb.2008.09.017
- Moreira, F.C., Boaventura, R.A.R., Brillas, E., Vilar, V.J.P., 2017. Electrochemical advanced

oxidation processes: A review on their application to synthetic and real wastewaters. *Appl. Catal. B Environ.* 202, 217–261. doi:10.1016/j.apcatb.2016.08.037

Murugananthan, M., Latha, S.S., Bhaskar Raju, G., Yoshihara, S., 2011. Role of electrolyte on anodic mineralization of atenolol at boron doped diamond and Pt electrodes. *Sep. Purif. Technol.* 79, 56–62. doi:10.1016/j.seppur.2011.03.011

O'Neill, C., Hawkes, F.R., Hawkes, D.L., Lourenço, N.D., Pinheiro, H.M., Delgado, W., 1999. Colour in textile effluents - Sources, measurement, discharge consents and simulation: A review. *J. Chem. Technol. Biotechnol.* 74, 1009–1018. doi:10.1002/(SICI)1097-4660(199911)74:11<1009::AID-JCTB153>3.0.CO;2-N

Oller, I., Malato, S., Sánchez-Pérez, J. a, 2011. Combination of Advanced Oxidation Processes and biological treatments for wastewater decontamination--a review. *Sci. Total Environ.* 409, 4141–66. doi:10.1016/j.scitotenv.2010.08.061

Palma-Goyes, R.E., Guzmán-Duque, F.L., Peñuela, G., González, I., Nava, J.L., Torres-Palma, R. A, 2010. Electrochemical degradation of crystal violet with BDD electrodes: effect of electrochemical parameters and identification of organic by-products. *Chemosphere* 81, 26–32. doi:10.1016/j.chemosphere.2010.07.020

Panizza, M., Cerisola, G., 2009. Direct and mediated anodic oxidation of organic pollutants. *Chem. Rev.* 109, 6541–69. doi:10.1021/cr9001319

Pereira, G.F., Rocha-Filho, R.C., Bocchi, N., Biaggio, S.R., 2012. Electrochemical degradation of bisphenol A using a flow reactor with a boron-doped diamond anode. *Chem. Eng. J.* 198–199, 282–288. doi:10.1016/j.cej.2012.05.057

Pieczynska, A., Ofiarska, A., Borzyszkowska, A.F., Białk-Bielińska, A., Stepnowski, P., Stolte, S., Siedlecka, E.M., 2015. A comparative study of electrochemical degradation of imidazolium and pyridinium ionic liquids: A reaction pathway and ecotoxicity evaluation. *Sep. Purif. Technol.* doi:10.1016/j.seppur.2015.10.045

Samet, Y., Agengui, L., Abdelhédi, R., 2010. Electrochemical degradation of chlorpyrifos pesticide in aqueous solutions by anodic oxidation at boron-doped diamond electrodes.



Chem. Eng. J. 161, 167–172. doi:10.1016/j.cej.2010.04.060

Sanroman, M.A., Pazos, M., Ricart, M.T., Cameselle, C., 2004. Electrochemical decolourisation of structurally different dyes. *Chemosphere* 57, 233–239.
doi:10.1016/j.chemosphere.2004.06.019

Santos, V., Morão, A., Pacheco, M.J., Ciriaco, L., Lopes, A., 2008. Electrochemical degradation of azo dyes on bdd : effect of chemical structure and operating conditions on the combustion efficiency 18, 193–204.

Siedlecka, E.M., Mroziak, W., Kaczyński, Z., Stepnowski, P., 2008. Degradation of 1-butyl-3-methylimidazolium chloride ionic liquid in a Fenton-like system. *J. Hazard. Mater.* 154, 893–900. doi:10.1016/j.jhazmat.2007.10.104

Siedlecka, E.M., Stolte, S., Nienstedt, A., Ossowski, T., Stepnowski, P., 2013. Electrocatalytic Oxidation of 1-Butyl-3-Methylimidazolium Chloride : Effect of the Electrode Material 8, 5560–5574.

Soloman, P.A., Basha, C.A., Velan, M., Ramamurthi, V., Koteeswaran, K., Balasubramanian, N., 2009. Electrochemical Degradation of Remazol Black B Dye Effluent. *CLEAN - Soil, Air, Water* 37, 889–900. doi:10.1002/clen.200900055

Tsantaki, E., Velegraki, T., Katsaounis, A., Mantzavinos, D., 2012. Anodic oxidation of textile dyehouse effluents on boron-doped diamond electrode. *J. Hazard. Mater.* 207–208, 91–96.
doi:10.1016/j.jhazmat.2011.03.107

Velegraki, T., Balayiannis, G., Diamadopoulou, E., Katsaounis, A., Mantzavinos, D., 2010. Electrochemical oxidation of benzoic acid in water over boron-doped diamond electrodes: Statistical analysis of key operating parameters, kinetic modeling, reaction by-products and ecotoxicity. *Chem. Eng. J.* 160, 538–548. doi:10.1016/j.cej.2010.03.065

Wächter, N., Pereira, G.F., Rocha, R.C., Bocchi, N., Biaggio, S.R., 2015. Comparative Electrochemical Degradation of the Acid Yellow Anodes in a Flow Reactor 10, 1361–1371.

Yavuz, Y., Canan, G., Bakır, O., 2007. Electrochemical degradation and toxicity reduction of C . I . Basic Red 29 solution and textile wastewater by using diamond anode 145, 100–108.

doi:10.1016/j.jhazmat.2006.10.090

Captures of figures

Fig. 1. Schematic view of undivided a) and divided b) flow reactor (1- reservoir, 2- peristaltic pump, 3- electrochemical cell, 4- BDD anode, 5- stainless steel cathode, 6- Nafion membrane)

Fig. 2. The degradation rate of Ruby F-2B during electrochemical oxidation at a current density of 8.8 mA cm^{-2} , the flow rate of 0.6 L h^{-1} , and pH 3.0 in the divided and undivided flow reactors

Fig. 3. The degradation rate of Ruby F-2B (a) and the amount of hydroxyl radicals generated (b) during electrochemical oxidation at current densities of 8.8 mA cm^{-2} , 6.6 mA cm^{-2} , 3.5 mA cm^{-2} ; the flow rate of 0.6 L h^{-1} , and pH 3.0 in a divided cell flow reactor

Fig. 4. The degradation rate of Ruby F-2B during electrochemical oxidation at a current density of 8.8 mA cm^{-2} , the flow rate 0.6 L h^{-1} , and the pH values of 3.0, 7.0, 9.0 and 12.0 in a divided cell flow reactor

Fig. 5. The degradation rate of the investigated dyes (50 mg L^{-1}) during electrochemical oxidation at a current density of 8.8 mA cm^{-2} , the flow rate of 0.6 L h^{-1} , and pH 3.0 in a divided cell flow reactor

Fig. 6. UV-Vis spectra of the dyes (Ruby F-2B (a), Red D-8B (b), Black DN (c), Blue D-5RN (d), Yellow D-5GN (e)) for different electrochemical oxidation times at a current density of 8.8 mA cm^{-2} , the flow rate of 0.6 L h^{-1} , and pH 3.0 in a divided cell flow reactor

Fig. 7. The degradation rate of the investigated dyes (50 mg L^{-1}) in an electrolyte and textile wastewater during electrochemical oxidation at a current density of 8.8 mA cm^{-2} , the flow rate of 0.6 L h^{-1} , and the pH values of 12.0 and 9.0 (Ruby F-2B) in a divided cell flow reactor



Captures of Tables

Table 1. The properties and chemical structure of helactine azo dyes

Table 2. The values of rate constant, COD removal efficiency and current efficiency measured during the electrochemical oxidation of dyes under the following conditions: current density 8.8 mA cm^{-2} , flow rate 0.6 L h^{-1} , pH 3.0, divided reactor with a two-compartment cell

Table 1. Properties and chemical structures of helactine azo dyes

Black DN

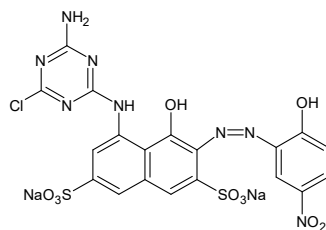
(Helectine D dye)

Molecular Formula

$C_{19}H_{11}Cl_1N_8Na_2O_{10}S_2$

Molecular Weight 656.5 g mol^{-1}

Max. wavelength 586 nm



Blue D-5RN

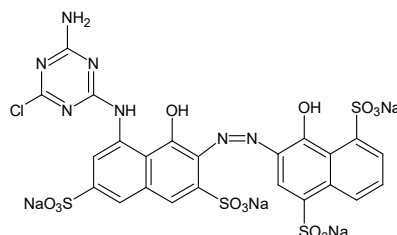
(Helectine D dye)

Molecular Formula

$C_{23}H_{12}Cl_1N_7Na_4O_{14}S_4$

Molecular Weight 865.5 g mol^{-1}

Max. wavelength 568 nm



Ruby F-2B

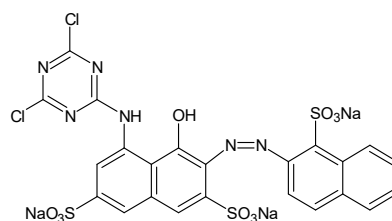
(Helectine F dye)

Molecular Formula

$C_{23}H_{11}Cl_2N_6Na_3O_{10}S_3$

Molecular Weight 767.0 g mol^{-1}

Max. wavelength 545 nm



Red D-8B

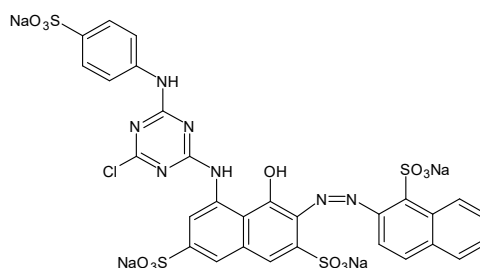
(Helectine D dye)

Molecular Formula

$C_{29}H_{16}Cl_1N_7Na_4O_{13}S_4$

Molecular Weight 925.5 g mol^{-1}

Max. wavelength 547 nm



**Yellow D-5GN
(Helectine D dye)**

Molecular Formula

$C_{25}H_{15}Cl_3N_9Na_3O_{10}S_3$

Molecular Weight 872.5 g mol^{-1}

Max. wavelength 406 nm

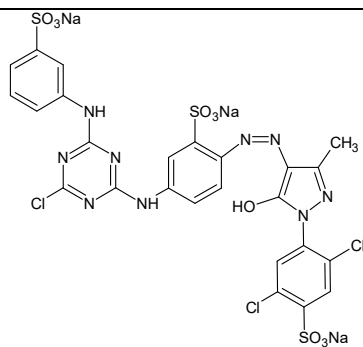


Table 2. Rates constant values, COD removal efficiency and current efficiency of dyes electrochemical oxidation in following conditions: current density 8.8 mA cm⁻², the flow rate 0.6 L h⁻¹, the pH 3.0, divided reactor for two compartments cell

	k (R ²) (min ⁻¹)	Dye removal efficiency (%)	COD removal efficiency (%)	CE (%)	Oxidation potential (V)
Ruby F-2B	0.0057 (0.991)	94.9 (420 min)	86.3 (420 min)	27.0	1.11
Black DN	0.0044 (0.987)	97.0 (480 min)	93.4 (480 min)	20.7	1.16
Red D-8B	0.0076 (0.988)	94.8 (300 min)	95.7 (300 min)	37.5	1.06
Blue D-5RN	0.0271 (0.936)	98.9 (120 min)	99.1 (120 min)	92.1	0.75
Yellow D-5RN	0.0092 (0.981)	86.8 (180 min)	97.3 (180 min)	60.9	0.99

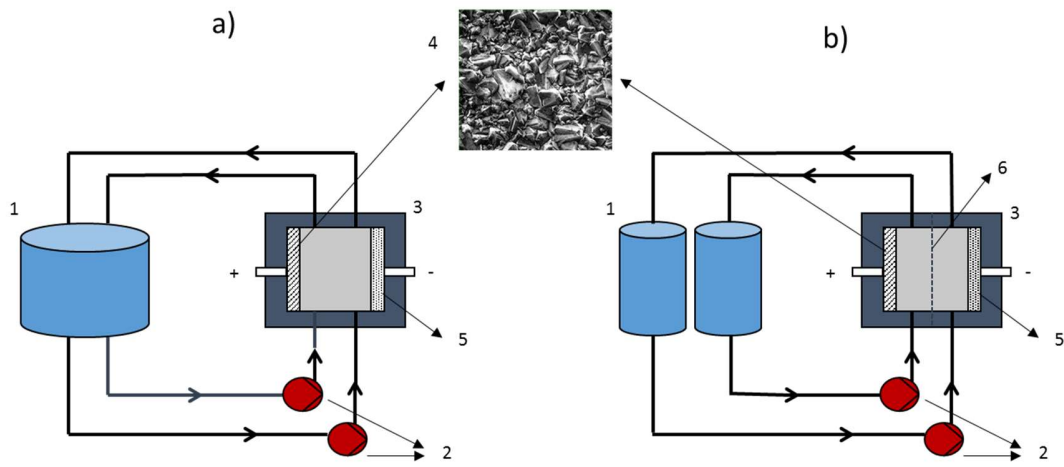


Fig. 1.

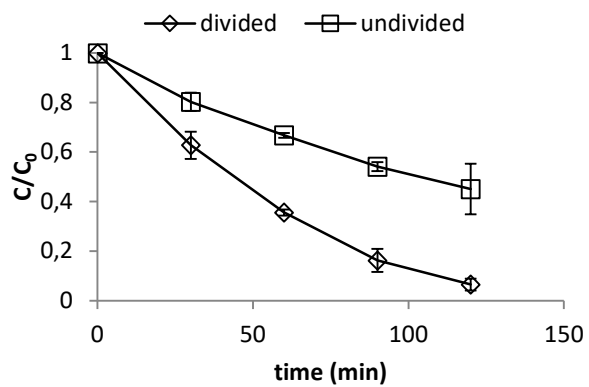


Fig 2.

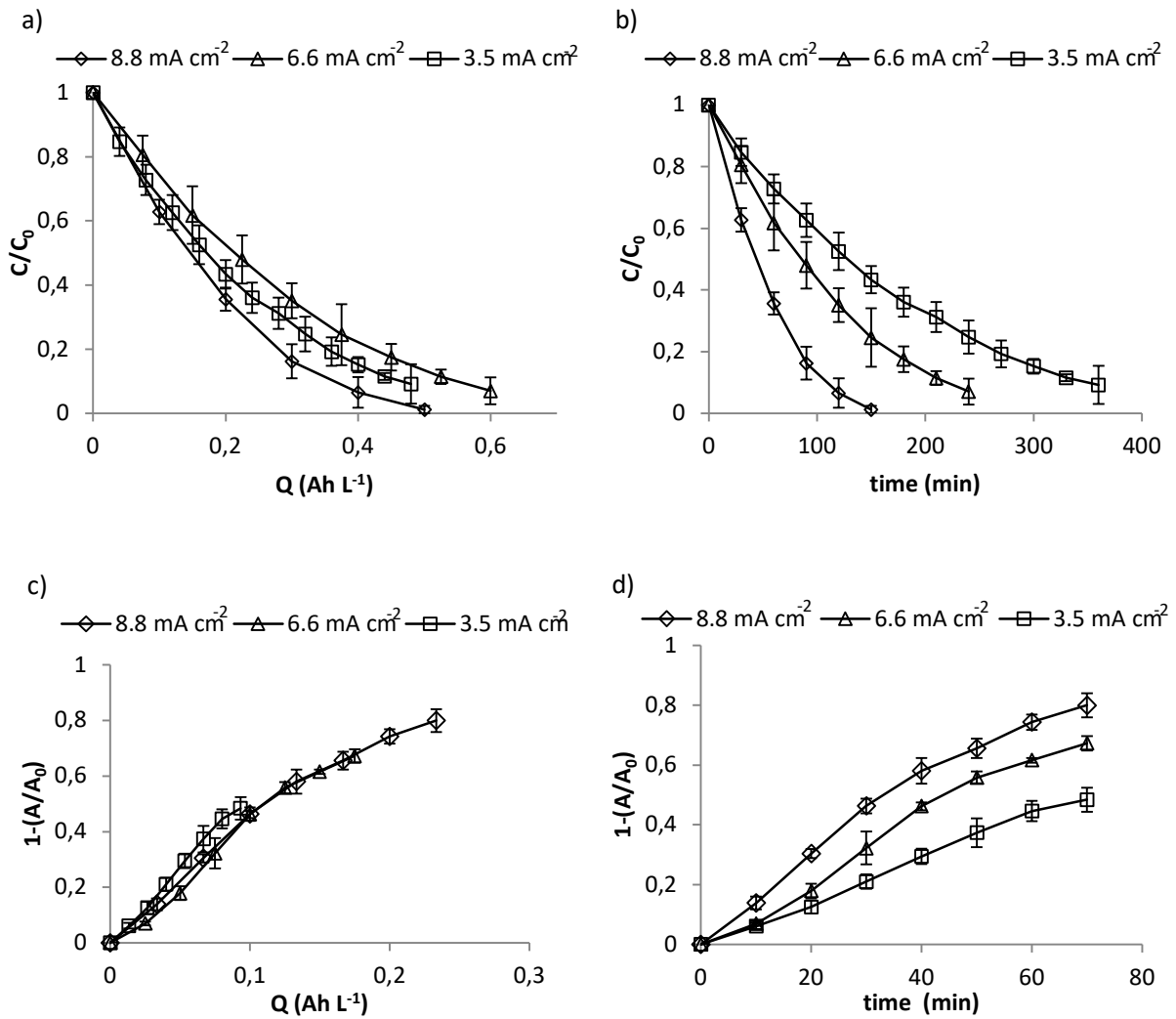


Fig 3.

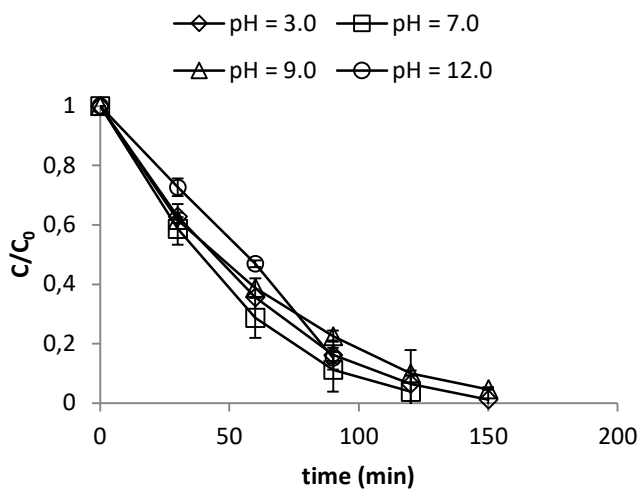


Fig 4.

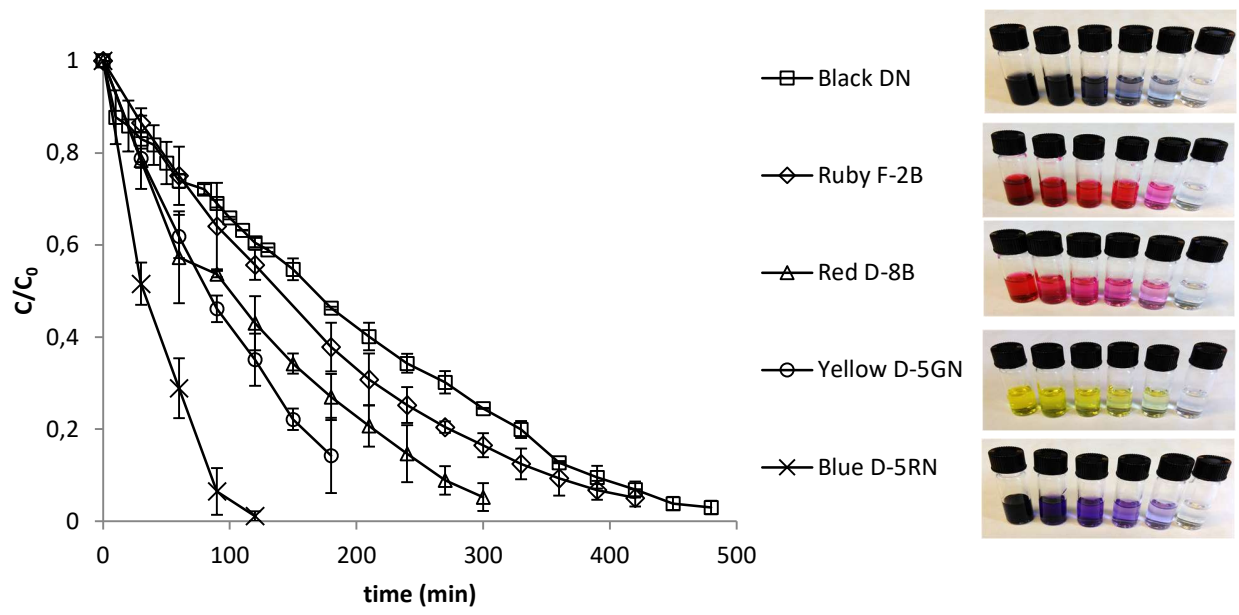
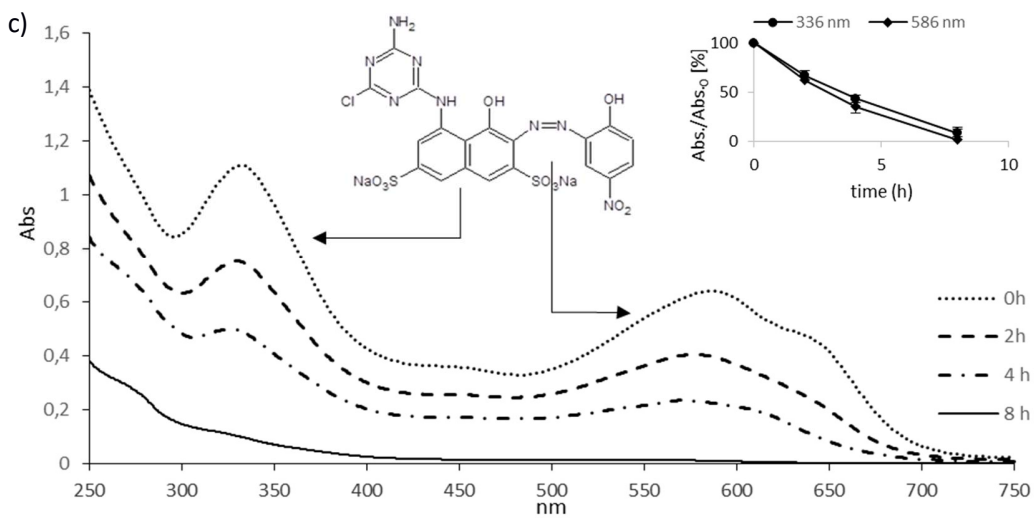
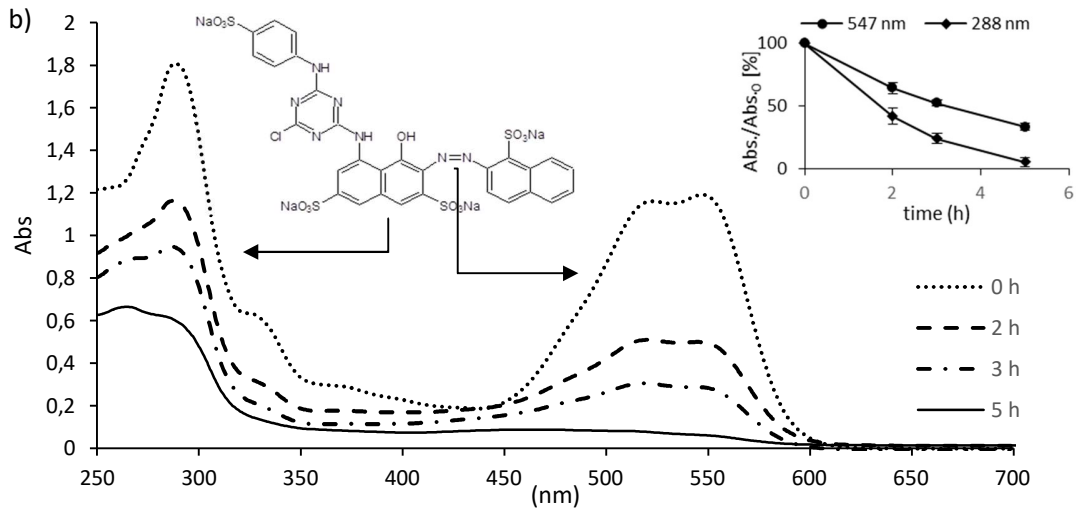
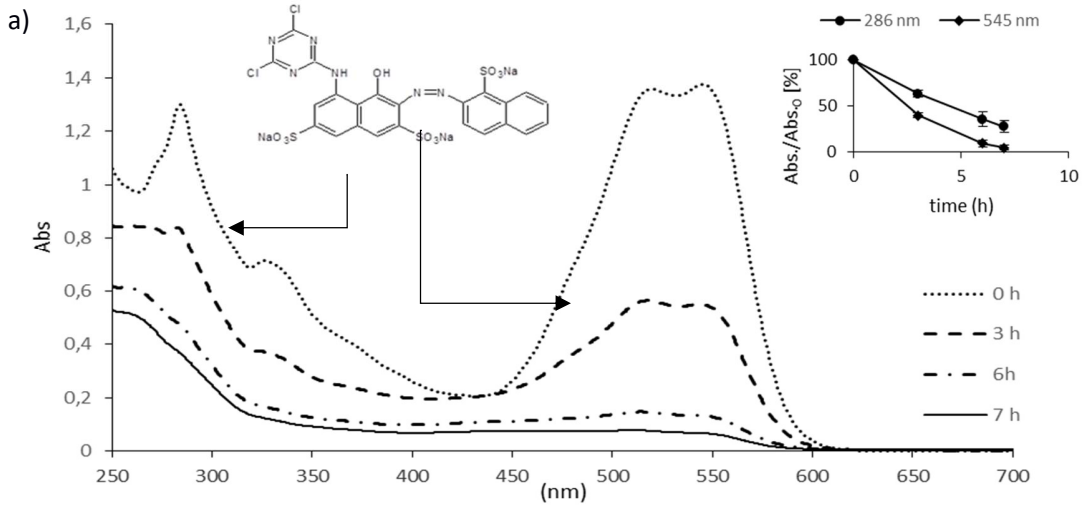


Fig 5.



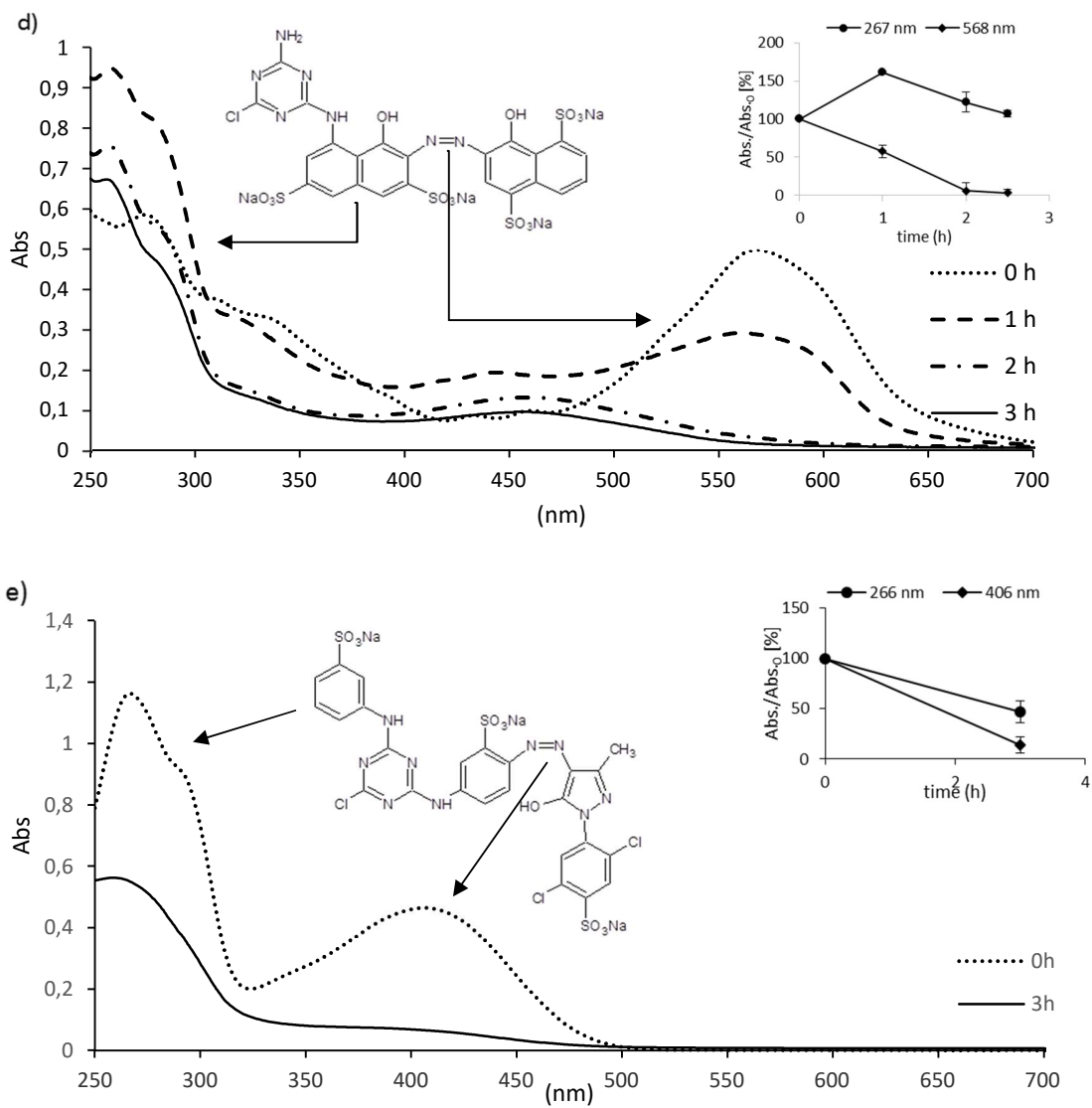
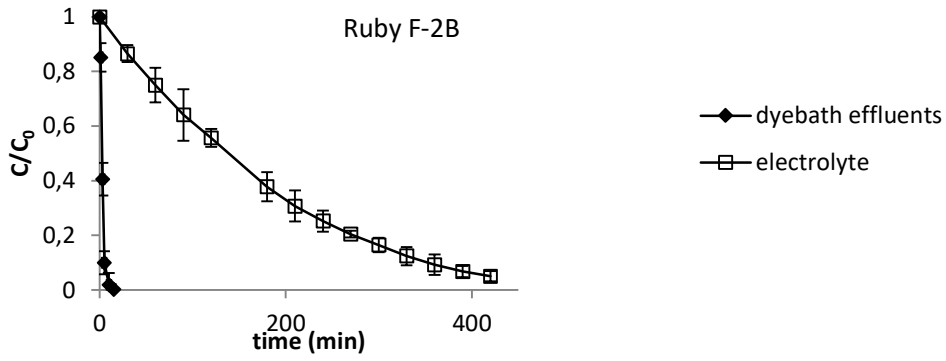


Fig 6.

Dye from group F



Dyes from group D

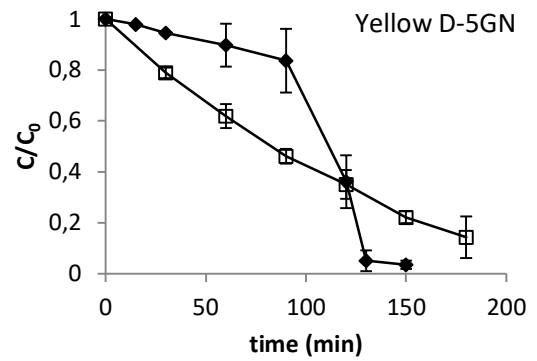
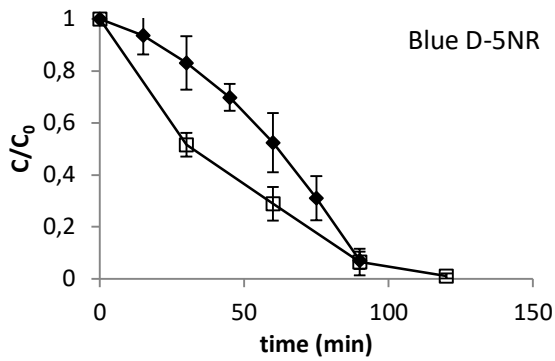
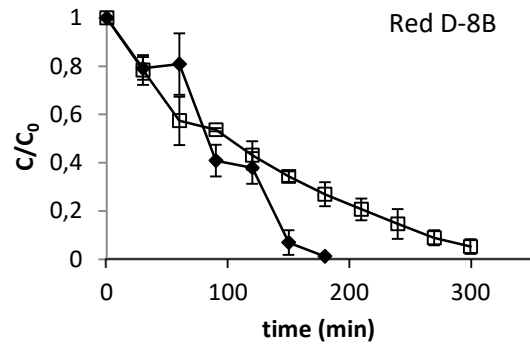
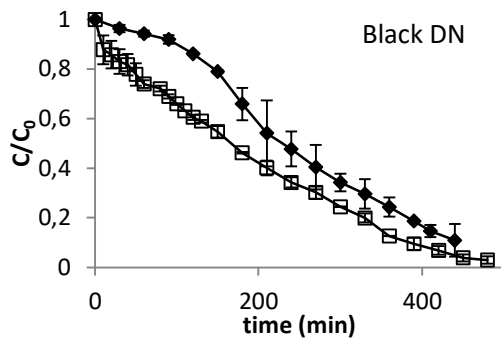


Fig 7.

Graphic abstract

